

Weak interaction rates involving  $^{12}\text{C}$ ,  $^{14}\text{N}$ , and  $^{16}\text{O}$ 

N. Auerbach

*Raymond and Beverly Sackler Faculty of Sciences, School of Physics and Astronomy, Tel Aviv University, Ramat Aviv, Tel Aviv 69978, Israel*

B. A. Brown

*Department of Physics and Astronomy and National Superconducting Cyclotron Laboratory, Michigan State University, East Lansing, Michigan 48824-1321*

(Received 7 September 2001; published 25 January 2002)

Muon capture and neutrino scattering cross sections in  $^{12}\text{C}$ ,  $^{14}\text{N}$ , and  $^{16}\text{O}$  are calculated within a large shell-model basis. The effects of quenching of the isovector strength on these quantities are studied.

DOI: 10.1103/PhysRevC.65.024322

PACS number(s): 21.60.Cs, 27.20.+n, 25.30.Pt, 23.40.-s

## I. INTRODUCTION

One of the outstanding problems in nuclear physics is the quenching of Gamow-Teller (GT) strength in nuclei. The discovery that a large part of the GT strength (about 40%) is missing from the main peak was made more than 20 years ago. The studies of  $\beta$  decay [1] and  $(p,n)$  reactions [2] failed to find the full strength given by the sum rule

$$S_- - S_+ = 3(N - Z), \quad (1)$$

where

$$S_{\pm} = \sum_n |\langle n | \sum_{i=1}^A \sigma(i) t_{\pm}(i) | 0 \rangle|^2, \quad (2)$$

and  $t_{\pm}$  are the isospin raising and lowering single-particle operators. Two main proposals were made to explain this puzzling quenching of the GT strength; (1) the missing strength is removed to the very high excitation energy of about 300 MeV above the ground state due to the process in which a nucleon is transformed into a  $\Delta_{33}$  resonance, or more precisely the GT strength is removed due to the interaction with the  $\Delta N^{-1}$  ( $\Delta$ -nucleon hole) configuration; (2) the missing GT strength is depleted by short-range correlations and moved to an excitation energy of up to 100 MeV above the main peak. Of course a combination of the two scenarios is also a possibility. Recent  $(p,n)$  experiments in heavy nuclei [3] favor the second possibility, but these have to be supported by additional studies before the resolution of the missing strength puzzle can be established fully. Analysis of GT transition and isoscalar magnetic moment data in the  $sd$  shell [4] indicates that the quenching factor in the GT matrix element is given approximately by  $\gamma = (1 - \delta_{c.m.} - \delta_{\Delta})$ , where  $\delta_{c.m.} = 0.16$  is the contribution from higher-order configuration mixing and  $\delta_{\Delta} = 0.08$  is the contribution from  $\Delta_{33}$  admixtures. The GT strength is reduced by the factor  $\gamma^2 = 0.58$ .

In addition to the  $\beta$  decay, other weak processes may probe the quenching of GT strength ( $L=0$ ) or more generally the spin-isospin strength for multipolarity  $L$ . Among such weak processes are the  $\mu^-$  capture and the charged-current (CC) neutrino scattering on nuclei. In the present

paper, we study the role of quenching of the spin-isospin response has on these two processes using large-basis shell-model calculations. In Ref. [5] the issue of quenching of the spin-isospin strength on weak interaction processes has been studied in a limited manner. Here we extend the calculation to  $^{14}\text{N}$  and  $^{16}\text{O}$  using full  $(0+1+2+3)\hbar\omega$  shell-model basis. In addition, we investigate the role of the  $sdg$  shell that has not previously been included in the shell-model basis.

## II. THE WEAK-INTERACTION PROCESSES

First, we direct our attention to  $\mu^-$  capture on nuclei. This subject is not new. Measurements of exclusive and inclusive  $\mu^-$  capture started in the 1960s and continue today (see Ref. [6] for a review). Calculations of the  $\mu^-$  capture rates followed. The inclusive cross sections have been treated either in a phenomenological way [7] or using the TDA and RPA [8]. Shell-model calculations of inclusive  $\mu^-$  capture did not exist until recently. Only in the last several years in the context of neutrino-nucleus interactions studies have there been several shell-model calculations of these capture rates. None of the above calculations have addressed fully the question of quenching of the spin-isospin response in nuclei. The early RPA results [8] of the inclusive rates were in agreement with experiment and it seemed that there was no need for quenching. This was somewhat surprising. In other strong-interaction reactions such as  $(p,n)$  and  $(^3\text{He},t)$ , etc., the GT strength appeared to be quenching considerably. But for the higher multiplicities ( $L=1$ ,  $L=2$ , etc.) in the spin-isospin response the question of whether there is quenching has not been answered.

Another class of weak processes that are able to probe the spin-isospin response are neutrino reactions on nuclei. In recent years several experiments were performed with laboratory produced electron ( $\nu_e$ ) and muon ( $\nu_{\mu}$ ) neutrinos using the  $^{12}\text{C}$  nucleus as a target [9,10]. The charged-current reactions  $^{12}\text{C}(\nu_e, e^-)^{12}\text{N}$  and  $^{12}\text{C}(\nu_{\mu}, \mu^-)^{12}\text{N}$  both exclusive (to the  $^{12}\text{N} 1^+$  ground state) and inclusive (to all final states) have provided additional information about the spin-isospin response of the  $^{12}\text{C}$  nucleus. The  $^{12}\text{C}(\nu_e, e^-)^{12}\text{N}$  reaction was done with the flux of neutrinos obtained from the decay at rest (DAR) of muons and pions while the  $^{12}\text{C}(\nu_{\mu}, \mu^-)^{12}\text{N}$  reaction was done with the decay in flight (DIF) neutrinos.

TABLE I. Results for cross sections, rates, and  $B(\text{GT})$  values. The units for  $\langle\bar{\sigma}\rangle(\text{DAR})$  are  $10^{-42}$  cm<sup>2</sup>, the units for  $\langle\bar{\sigma}\rangle(\text{DIF})$  are  $10^{-40}$  cm<sup>2</sup>, and the units for  $\Lambda$  are  $10^3/\text{s}$ . The experimental values are compared to the calculated values based on the  $0\hbar\omega$  and  $(0+2)\hbar\omega$  ground-state wave functions.

Process	Final states	Expt.	$0\hbar\omega$ Gs	$(0+2)\hbar\omega$ Gs	$0\hbar\omega$ Gs $\times 0.64$
$\langle\bar{\sigma}\rangle(\text{DAR})$ $^{16}\text{O}(\nu_e, e^-)^{16}\text{F}$	+ Parity		0.6		0.4
	- Parity		16.3	11.5	10.4
	Total		16.9		10.8
$\langle\bar{\sigma}\rangle(\text{DIF})$ $^{16}\text{O}(\nu_\mu, \mu^-)^{16}\text{F}$	+ Parity		13.1		8.4
	- Parity		15.8	11.3	10.1
	- Parity ( <i>sdg</i> )		5.1		3.3
	Total		34.1		21.8
$\Lambda$ $\mu^-$ capture $^{16}\text{O}$ to $^{16}\text{N}$	+ Parity		23		15
	- Parity		139	102	89
	Total	$102.5 \pm 1.0$ (Ref. [6])	162		104
$\langle\bar{\sigma}\rangle(\text{DAR})$ $^{14}\text{N}(\nu_e, e^-)^{14}\text{O}$	+ Parity		33.0		21.1
	- Parity		11.8		7.6
	Total		45.1		28.9
$\langle\bar{\sigma}\rangle(\text{DIF})$ $^{14}\text{N}(\nu_\mu, \mu^-)^{14}\text{O}$	+ Parity		11.9		7.6
	- Parity		14.1		9.0
	- Parity ( <i>sdg</i> )		3.0		1.9
	Total		29.0		19.6
$\Lambda$ $\mu^-$ capture $^{14}\text{N}$ to $^{14}\text{C}$	+ Parity		35		22
	- Parity		73		46
	Total	$66 \pm 5$ (Ref. [33])	108		68
$\langle\bar{\sigma}\rangle(\text{DAR})$ $^{12}\text{C}(\nu_e, e^-)^{12}\text{N}$	$1^+$ Gs	$9.1 \pm 0.4 \pm 0.9$ (Refs. [9,10])	14.6		9.3
	+ Parity (other)		0.7		0.4
	- Parity		8.4		5.4
	Total	$14.1 \pm 1.2$ (Refs. [9,10])	23.7		15.1
$\langle\bar{\sigma}\rangle(\text{DIF})$ $^{12}\text{C}(\nu_\mu, \mu^-)^{12}\text{N}$	$1^+$ Gs	$0.66 \pm 0.14$ (Ref. [10])	1.4		0.9
	+ Parity (other)		9.9		6.3
	- Parity		15.3		9.8
	- Parity ( <i>sdg</i> )		3.4		2.2
	Total	$12.4 \pm 0.3 \pm 1.8$ (Ref. [10])	30.0		19.2
$\Lambda$ $\mu^-$ capture $^{12}\text{C}$ to $^{12}\text{B}$	$1^+$ Gs	$6.0 \pm 0.4$ (Ref. [6])	9.4		6.0
	+ Parity (other)		5.7		3.6
	- Parity		37.3		23.9
	Total	$37.9 \pm 0.5$ (Ref. [6])	52.4		33.5
$B(\text{GT})$ for $^{12}\text{C}$ to $^{12}\text{N}$	$1^+$ Gs	$0.99 \pm 0.01$ (Ref. [29])	1.45		0.93
$B(\text{GT})$ for $^{12}\text{C}$ to $^{12}\text{B}$	$1^+$ Gs	$0.87 \pm 0.01$ (Ref. [29])	1.45		0.93

The flux of DAR neutrinos contains electron neutrinos with a maximum energy of 50 MeV. The DIF  $\nu_\mu$  flux has a maximum neutrino energy of about 300 MeV, but the threshold for the  $^{12}\text{C}(\nu_\mu, \mu^-)^{12}\text{N}$  reaction is about 120 MeV. One should also note that the flux of  $\nu_\mu$  neutrinos drops steeply with energy above 150 MeV [10].

The experimental results for the DIF and DAR neutrino- $^{12}\text{C}$  flux-averaged cross sections are given in Table I. Note

that in the case of the  $\nu_\mu$  neutrinos the exclusive cross section to the  $^{12}\text{N}$  ground state is a very small fraction of the inclusive cross section, while for the  $\nu_e$  neutrinos the exclusive cross section is more than half of the inclusive one. The reason is simply that the  $\nu_e$  cross sections are due to the DAR neutrinos that contain only a low flux of neutrinos that can excite high-lying states and therefore the exclusive cross section is large compared to the inclusive one.

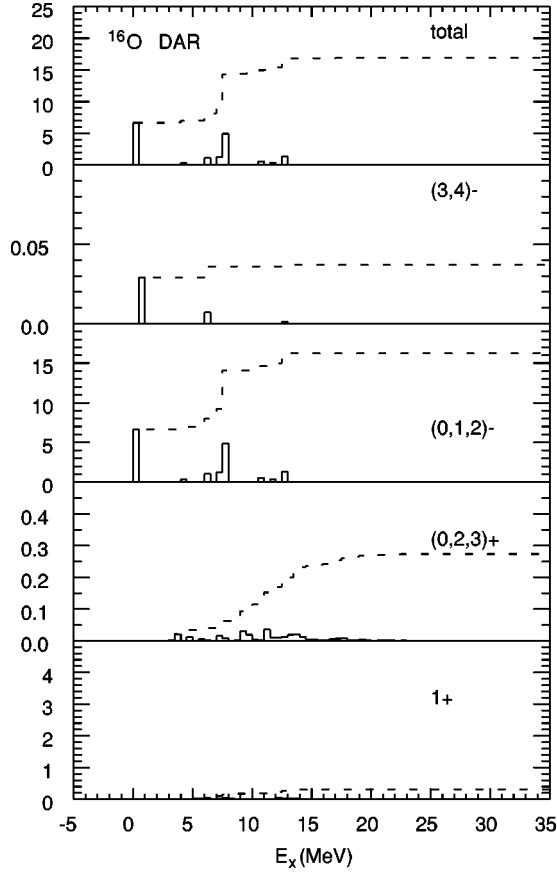


FIG. 1. Contributions to the  $^{16}\text{O} \rightarrow ^{16}\text{F}$  DAR cross section in the  $0\hbar\omega$  ground-state model space. The units are  $10^{-42} \text{ cm}^2$ . The contribution of the individual final states binned over energy intervals of 0.5 MeV are shown by the solid histogram. The dashed line is a running sum of the total. Contributions from individual final states with the spins and parities indicated are shown in the lower panels, while the total from all final states is shown in the top panel.

In this paper, we will calculate in addition to the  $^{12}\text{C}$  nucleus also  $^{14}\text{N}$  and  $^{16}\text{O}$ . In  $^{14}\text{N}$  and  $^{16}\text{O}$  only the  $\mu^-$  capture rates are known experimentally. The CC neutrino cross sections have not been measured. The additional experimental information we will consider is the GT  $\beta$ -decay transition from the  $^{12}\text{B}$  and  $^{12}\text{N}$  ground state to the  $^{12}\text{C}$  ground state.

### III. CALCULATIONS OF $\mu^-$ CAPTURE AND CC NEUTRINO CROSS SECTIONS

Using the one-body transition densities from the large-basis shell-model calculation we compute the  $\mu^-$  capture rates and CC neutrino cross sections for  $^{12}\text{C}$ ,  $^{14}\text{N}$ , and  $^{16}\text{O}$ . The weak-interaction calculations were obtained with the computer codes by Towner [11] used in Ref. [12]. The contributions of the vector ( $V$ ), axial vector ( $A$ ), and induced pseudoscalar ( $P$ ) are evaluated without the need to employ approximations, details are given in Ref. [12]. For the CC cross sections the weak-interaction code carries out the average over the DAR and DIF neutrino fluxes [9,10].

The neutrino cross sections involve the nuclear matrix

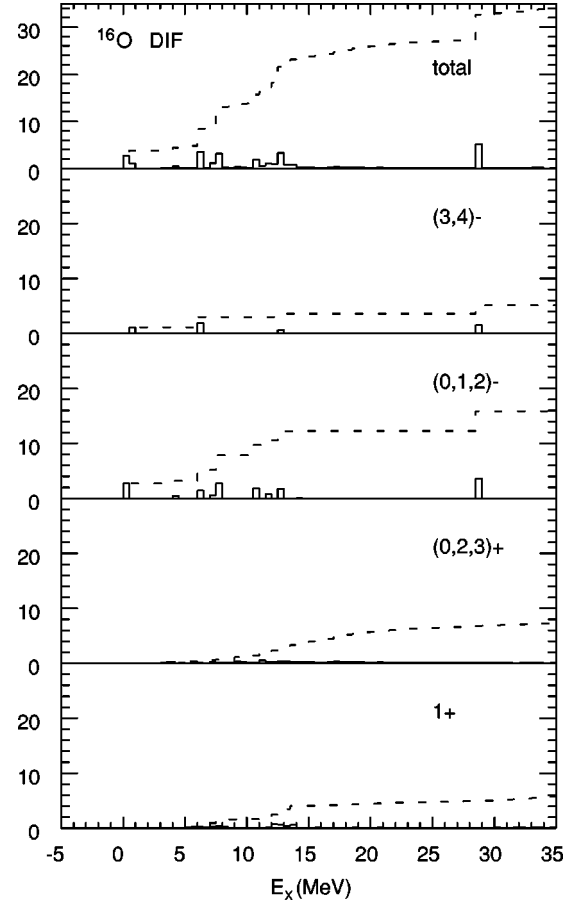


FIG. 2. Contributions to the  $^{16}\text{O} \rightarrow ^{16}\text{F}$  DIF cross section in the  $0\hbar\omega$  ground-state model space. The units are  $10^{-40} \text{ cm}^2$ . (See caption to Fig. 1.)

elements of the spin-independent  $[j_L(rq)Y_L t_-]$  and spin-dependent  $[j_L(qr)[Y_L \otimes \sigma]^J t_-]$  operators, where  $j_L$  is the spherical Bessel function of order  $L$ . For more details see Refs. [5,12]. After calculating the cross section for a neutrino energy  $E_\nu$  and for all scattering angles, one then integrates over the angles to get  $\sigma(E_\nu)$ . The flux averaged cross section

$$\langle \bar{\sigma} \rangle = \int \sigma(E_\nu) f(E_\nu) dE_\nu$$

is compared to experiment. The calculation of the cross section involves the coupling constants for vector ( $g_V$ ), axial vector ( $g_A$ ), and induced pseudoscalar ( $g_P$ ) weak currents. The quenching of the GT strength is often introduced operationally in terms of an effective axial vector coupling constant

$$\tilde{g}_A = g_A \gamma, \quad (3)$$

where  $\gamma$  is the amplitude quenching factor.

### IV. SHELL-MODEL CALCULATIONS OF THE MULTIPOLE STRENGTH DISTRIBUTION

The nuclear structure part of the calculation is performed in the framework of a large-basis shell model that includes

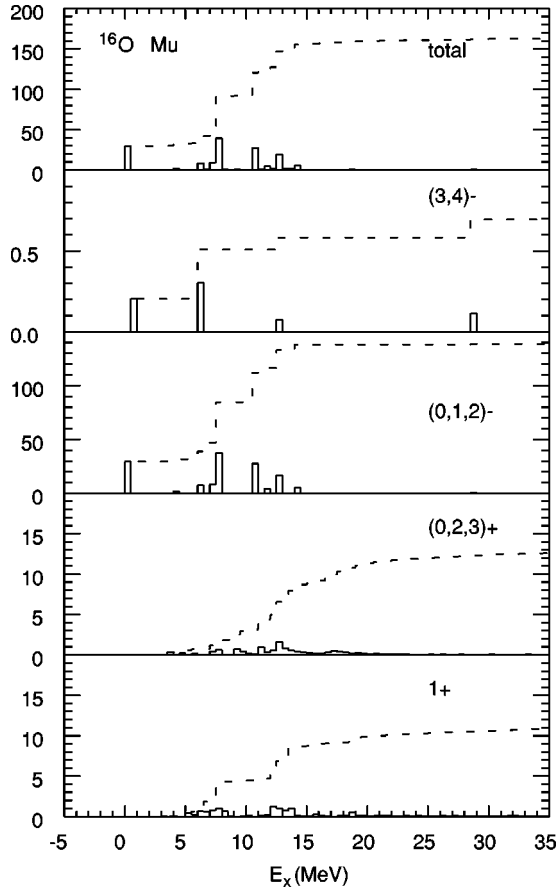


FIG. 3. Contributions to the  $^{16}\text{O} \rightarrow ^{16}\text{N} \mu^-$  capture rate in the  $0\hbar\omega$  ground-state model space. The units are  $10^3/\text{s}$ . (See caption to Fig. 1.)

the set of orbitals  $0s_{1/2}$ ,  $0p_{3/2}$ ,  $0p_{1/2}$ ,  $0d_{5/2}$ ,  $0d_{3/2}$ ,  $1s_{1/2}$ ,  $0f_{7/2}$ ,  $0f_{5/2}$ ,  $1p_{3/2}$ , and  $1p_{1/2}$ . (The contribution of higher orbitals will also be discussed.) We consider two model spaces. The simplest is one which can be easily be used for all light nuclei. The ground state is a  $0\hbar\omega$  configuration, and excited states are given by  $1\hbar\omega$  (negative parity) and  $2\hbar\omega$  (positive parity) configurations. The  $1\hbar\omega$  configurations include the giant dipole resonance that is dominated by  $0p \rightarrow 1s0d$  excitation, and the  $2\hbar\omega$  configurations include the giant quadrupole resonance that is dominated by  $0p \rightarrow 0f1p$  excitations. In the  $0\hbar\omega$  ground-state model, no mixing between the  $0\hbar\omega$  and  $2\hbar\omega$  excited states is allowed.

The  $0\hbar\omega$  ground state for  $^{16}\text{O}$  is just the closed-shell configuration, and  $0\hbar\omega$  for  $^{12}\text{C}$  is the full  $p$ -shell configuration. Interactions designed for this model space are MK [13], WBP [14] and WBT [14]. The results we discuss are similar for all three and we will give the details for WBP. This  $0\hbar\omega$  ground-state model space has been used for the analysis of electron scattering ( $e, e'$ ) data [15] and  $(p, n)$  [16,17],  $(p, p')$  [18], and  $(n, p)$  [19,20] reaction data on  $^{12}\text{C}$  and  $^{16}\text{O}$ .

An extended model space for  $^{16}\text{O}$  includes the admixture of  $2\hbar\omega$  in the ground state. To ensure the completeness of the final states with regard to one-body excitations in our model space we include up to  $3\hbar\omega$  in the final states. The off-diagonal interactions that were used to connect  $0\hbar\omega$  and

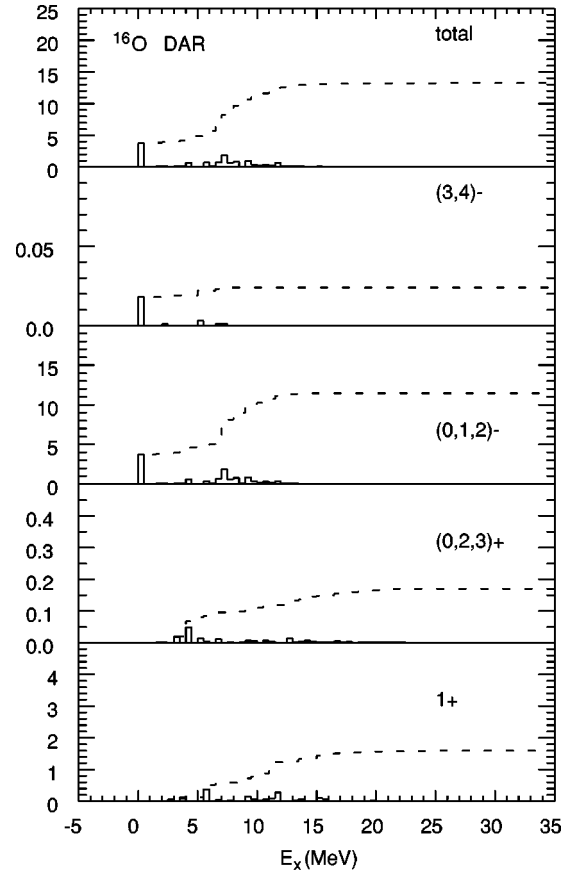


FIG. 4. Contributions to the  $^{16}\text{O} \rightarrow ^{16}\text{F}$  DAR cross section in the  $(0+2)\hbar\omega$  ground-state model space. The units are  $10^{-42} \text{ cm}^2$ . (See caption to Fig. 1.)

$2\hbar\omega$  (and  $1\hbar\omega$  and  $3\hbar\omega$ ) are taken from the CD-Bonn  $G$  matrix [21]. An example of the off-diagonal matrix element is  $\langle 0p, 0p | V | 1s0d, 1s0d \rangle$ . The WBP interaction should be renormalized to take into account the change of model space. Also there are energy shifts of the various  $\hbar\omega$  configuration for which one needs much higher  $\hbar\omega$  for convergence [22]. Nevertheless the effect of the off-diagonal interaction on the ground-state correlations should be realistic. The effect of  $2\hbar\omega$  ground-state admixtures is to give a significant RPA-type renormalization to the isovector excitations [23]. Thus, we use the extended model space to calculate the influence of the  $2\hbar\omega$  admixture on the total strength of the excitations with  $L=1, 2, 3, 4$ . The  $2\hbar\omega$  admixtures also allow for additional GT strength for  $^{16}\text{O}$  (and other nuclei) and we will comment on the importance of this.

In Ref. [12] excitations up to  $2\hbar\omega$  were used for  $^{12}\text{C}$  with extrapolations to  $3\hbar\omega$  and  $4\hbar\omega$ . In Ref. [5] up to  $3\hbar\omega$  excitations were included. The explicit introduction of  $3\hbar\omega$  is very important and will be discussed.

It is possible, but not easy, for us to carry out  $(0+1+2+3)\hbar\omega$  calculations for  $^{14}\text{N}$  and  $^{12}\text{C}$ . In contrast, calculations based on  $0\hbar\omega$  ground states with  $0, 1, 2\hbar\omega$  final states are possible for most light nuclei, and most of the structure details are already present at this level. Thus, our strategy will be to assume that the role of ground-state correlations beyond  $0\hbar\omega$  can be taken into account by effective opera-

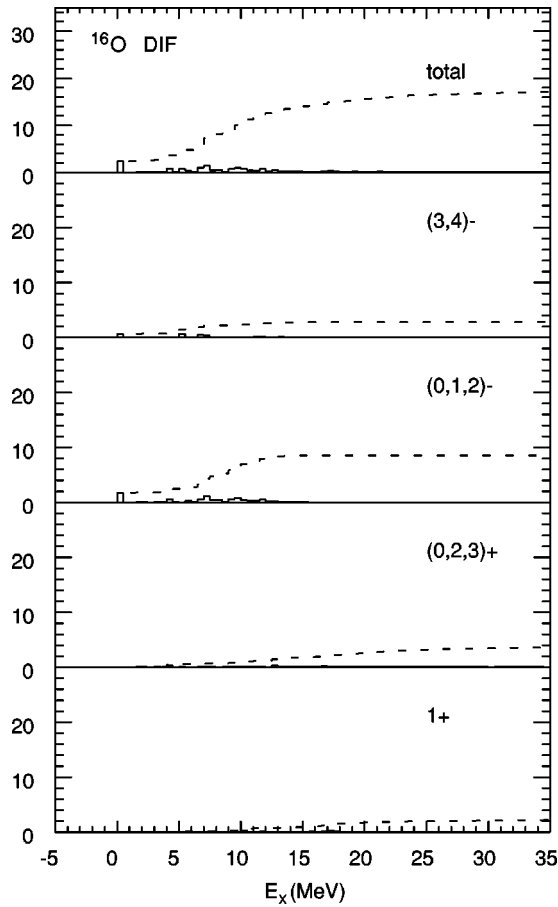


FIG. 5. Contributions to the  $^{16}\text{O} \rightarrow ^{16}\text{F}$  DIF cross section in the  $(0+2)\hbar\omega$  ground-state model space. The units are  $10^{-40} \text{ cm}^2$ . (See caption to Fig. 1.)

tors. In this paper, we will show that the simplest possible choice of an overall renormalization can account for most of the experimental data. As we will discuss below, this renormalization may have several sources including the long-range RPA-type and short-range-interaction correlations in the ground state.

We and others [5,12] have investigated the importance of the various  $L$  contributions to the DAR, DIF, and  $\mu^-$  capture processes. For DAR the  $L=0,1$  components are most important with higher  $L$ 's giving only a few percent more. For  $\mu^-$  capture up to  $L=2$  is needed. And for DIF up to  $L=3$  is needed with  $L=4$  adding less than about 5% to the cross section. With regard to these important  $L$  values our model space includes most of the important excitations. The most important ones outside the model space are the  $L=1,3$  excitations from the  $0p$  shell to the  $2s-1d-0g$  shell. We have estimated these contributions by explicitly adding to the one-body transition density all possible terms that represent the excitation from the  $0p$  shell to the  $2s-1d-0g$  orbitals, and have placed them all at the same excitation energy of about  $3\hbar\omega$ . In reality these transitions will be mixed with those in the model space so that the strength will be spread over a much larger energy range. But the total strength should be about the same and the high-energy DIF process is sensitive

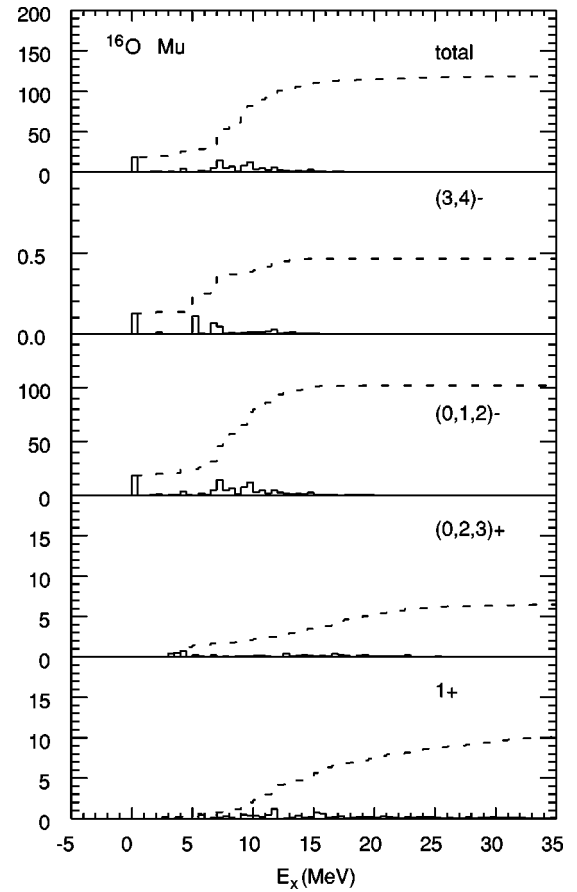


FIG. 6. Contributions to the  $^{16}\text{O} \rightarrow ^{16}\text{N}$   $\mu^-$  capture rate in the  $(0+2)\hbar\omega$  ground-state model space. The units are  $10^3/\text{s}$ . (See caption to Fig. 1.)

mainly to the total strength and not to the details of the distribution.

The calculations were carried out with the shell-model code OXBASH [24]. Up to about 400 final state eigenvectors for a given  $J$  value were calculated to ensure that the strength function of the one-body operator was exhausted. Harmonic-oscillator radial wave functions were used with  $b = 1.64 \text{ fm}$  for  $^{12}\text{C}$  and  $^{14}\text{N}$  and  $b = 1.77 \text{ fm}$  for  $^{16}\text{O}$ . These values are based upon the rms charge radii of the ground states.

## V. DISCUSSION AND COMPARISON WITH EXPERIMENT

We start with a discussion of the two model spaces for  $^{16}\text{O}$ . The total reaction cross sections and  $\mu^-$  capture rate are given in Table I. Figures 1–3 show how the totals for the  $0\hbar\omega$  ground-state model are related to the individual excited states, both in terms of the individual contributions and in terms of the running sum. The peak that can be observed near 28 MeV in Figs. 2 and 3 is the  $3\hbar\omega$  contribution from the  $0p$  to  $2s-1d-0g$  orbits. It adds about 20% to the DIF cross section, but for DAR and  $\mu^-$  capture its contribution is small. The experimental inclusive  $\mu^-$  capture rate that is dominated by  $L=1$  is a factor of about 0.6 smaller than theory. This is consistent with the quenching observed for the

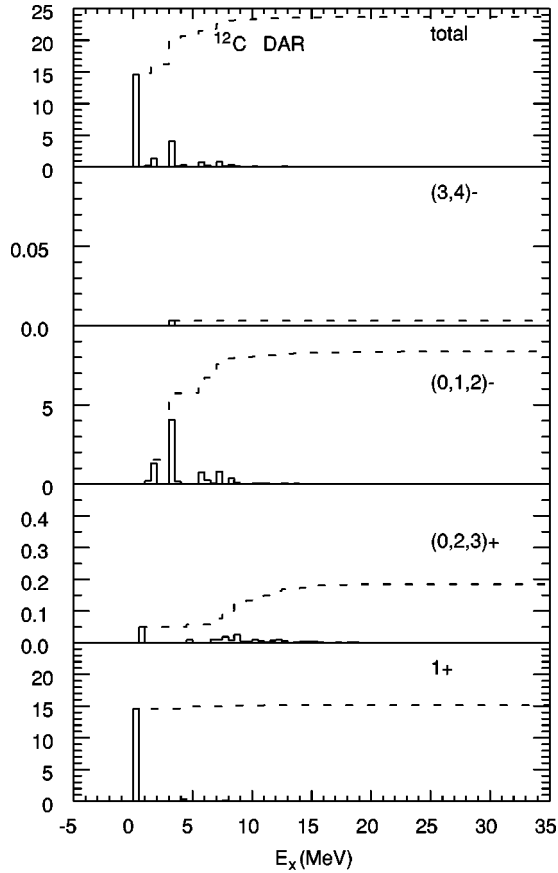


FIG. 7. Contributions to the  $^{12}\text{C} \rightarrow ^{12}\text{N}$  DAR cross section in the  $0\hbar\omega$  ground-state model space. The units are  $10^{-42} \text{ cm}^2$ . (See caption to Fig. 1.)

spin-dipole strength in the  $^{16}\text{O}(n,p)$  reaction [25] when analyzed with  $0\hbar\omega$  (closed-shell) ground-state wave function.

The  $(0+2)\hbar\omega$  ground-state results for  $^{16}\text{O}$  are given in Table I and Figs. 4–6. (These calculations do not include the  $2s-1d-0g$  shell contributions). There are several new features in the  $(0+2)\hbar\omega$  ground-state model. One is a reduction in the total strength that comes from an interference between the  $0\hbar\omega \rightarrow 1\hbar\omega$  and  $2\hbar\omega \rightarrow 1\hbar\omega$  contributions to the one-body matrix element. The sign of the effect is related to the repulsive nature of the isovector part of the Hamiltonian [23]. The  $2\hbar\omega$  admixture in the ground state is large (about 50%), and thus it is also important to include the  $3\hbar\omega$  final states that are required for the  $2\hbar\omega \rightarrow 3\hbar\omega$  excitations. We find that the  $2\hbar\omega$  mixture gives a uniform reduction of 0.70–0.73 for the negative-parity states independent of the excitation process. This reduction in strength is due to an absolute reduction in the total strength and not to a shift to higher excitation energy. (Without the explicit  $3\hbar\omega$  the reduction would have been about 0.30. It is not clear how much of the difference between 0.30 and 0.70 is included in the extrapolations presented in Ref. [12].) An evaluation of the effect  $(0+2)\hbar\omega$  ground state on the strength to positive-parity states would require  $4\hbar\omega$  final states that we do not include.

The value of the reduction depends upon the off-diagonal interaction that is the CD-Bonn  $G$  matrix in our case. There

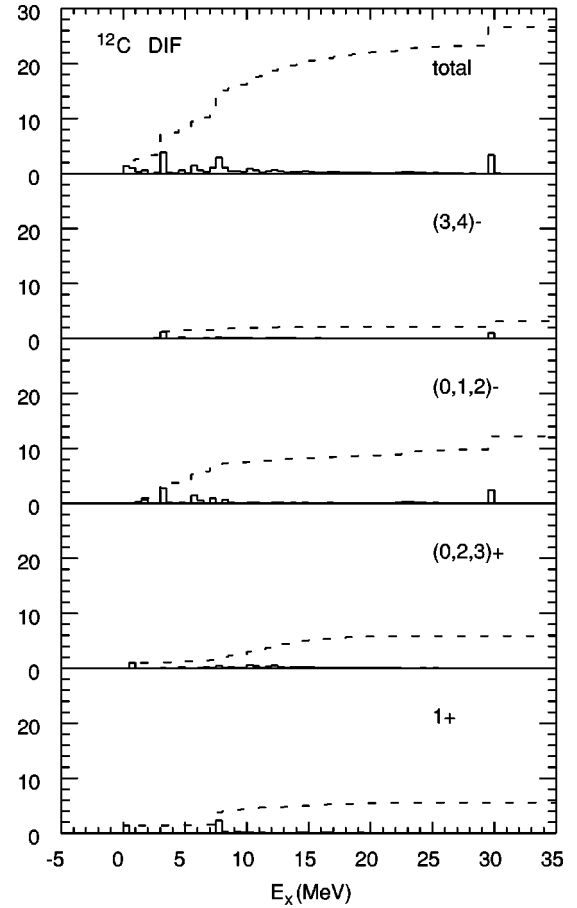


FIG. 8. Contributions to the  $^{12}\text{C} \rightarrow ^{12}\text{N}$  DIF cross section in the  $0\hbar\omega$  ground-state model space. The units are  $10^{-40} \text{ cm}^2$ . (See caption to Fig. 1.)

may be some renormalizations of the  $G$  matrix that will effect the reduction. Thus, we take the  $(0+2)\hbar\omega$  ground-state calculation as a qualitative measure of the size of the quenching due to long-range correlations (such as RPA), and make use of the observation that obtained quenching is independent of the excitation process. There may be other sources for changes in the theoretical value. As discussed in the Introduction, the reduction in the GT strength is attributed to a combination of higher-order configuration mixing and  $\Delta_{33}$  admixtures. The higher-order configuration mixing is related to the short-range (tensor) correlations in the bare nucleon-nucleon interaction [26]. These effects must also apply to high  $L$  values but they have never been fully evaluated. The effect of short-range correlations is also related to the reduction in the spectroscopic factors observed in  $(e,e'p)$  reactions that is attributed to short-range correlations [27]. The value for the spectroscopic factor reduction in  $^{12}\text{C}$  depends upon the reaction model used for  $(e,e'p)$  but ranges from 0.6 to 0.9 [28]. The  $(0+2)\hbar\omega$  ground-wave function for  $^{12}\text{C}$  gives a  $p$ -shell spectroscopic factor that is reduced only by 0.95 from the  $0\hbar\omega$  value.

It has been claimed that the loose binding of the excited states results in reduction of isovector strength. The use of loosely bound Woods-Saxon wave functions to represent an

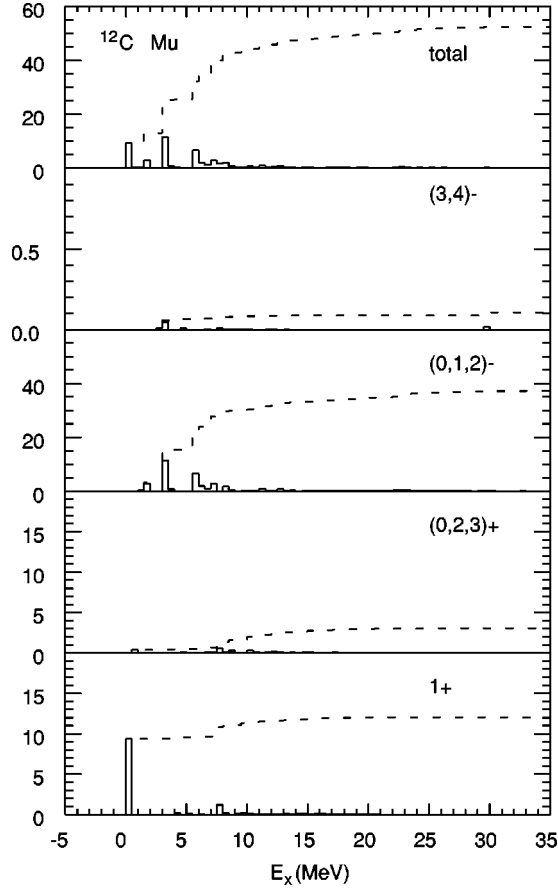


FIG. 9. Contributions to the  $^{12}\text{C} \rightarrow ^{12}\text{B} \mu^-$  capture rate in the  $0\hbar\omega$  ground-state model space. The units are  $10^3/\text{s}$ . (See caption to Fig. 1.)

approximation to the unbound single-particle states as used in Ref. [12] is problematical due to the nonorthogonality introduced by the different effective potential depths needed to bind the valence states. We feel that the use of oscillator approximation is better because it is numerically accurate and well defined. Part of the “quenching” we discuss may be related to the continuum nature of the excited states but a proper account is beyond our model and computational capabilities.

The only weak-interaction data in  $^{16}\text{O}$  with which we can compare is the total  $\mu^-$  capture rate. The  $0\hbar\omega$  ground-state theory can be brought into agreement with  $\mu^-$  capture by an overall reduction of about 0.64, which corresponds to a reduction in the amplitude by a factor of  $\gamma' = 0.80$ . The  $\mu^-$  capture contains both spin-dependent and spin-independent operators but is dominated by the spin-dipole part. It turns out that the value of  $\gamma'$  is similar to the factor by which the GT strength must be renormalized [the  $\gamma$  in Eq. (3)] in  $0\hbar\omega$  calculations of GT  $\beta$  decay in the  $p$  shell,  $\gamma = 0.82$  [29] and  $sd$  shell,  $\gamma = 0.76$  [1] nuclei.

Another effect of the  $(0+2)\hbar\omega$  ground state is to spread the isovector (spin-dependent and spin-independent) strength from a total of about eight states in the  $1\hbar\omega$  model (Figs. 1–3) over a total of about 50 states up to 15 MeV in excita-

TABLE II. Results for  $\mu^-$  capture rates to bound states. The theoretical results are based on the  $0\hbar\omega$  ground-state model and multiplied by  $(\gamma')^2 = 0.64$ . The data are from Refs. [6,33]. Note: As recommended by the authors [40], the rates obtained in Ref. [33] for all levels in  $^{14}\text{N}$  (except the 7.02 MeV  $2^+$ ) are renormalized up by a factor of 1.5 to agree with the total  $\gamma$ -ray yield obtained by Ref. [41]. For the 7.02 MeV  $2^+$  we use the average value recommended in Ref. [33].

Initial nucleus	Final nucleus	$J^\pi$	$E_x(\text{expt.})$ (MeV)	$\Lambda(\text{expt.})$ ( $10^3/\text{s}$ )	$E_x(\text{th})$ (MeV)	$\Lambda(\text{th})$ ( $10^3/\text{s}$ )
$^{16}\text{O}$	$^{16}\text{N}$	$2^-$	0.0	$8.0 \pm 1.2$	0.0	11.2
		$0^-$	0.12	$1.56 \pm 1.8$	0.02	3.0
		$3^-$	0.30	$< 0.09$	0.52	0.13
		$1^-$	0.40	$1.31 \pm 1.1$	0.47	4.7
$^{14}\text{N}$	$^{14}\text{C}$	$0^+$	0.0		0.0	0.3
		$1^-$	6.09	$1.2^{+0.6}_{-1.0}$	5.48	1.4
		$0^+$	6.59	$< 0.05$	4.68	0.0
		$3^-$	6.73	$1.4 \pm 0.5$	6.45	1.7
		$0^-$	6.90	$< 0.5$	7.15	0.4
		$2^+$	7.02	$4.4 \pm 0.6$	6.85	7.6 <sup>a</sup>
		$2^-$	7.34	$< 0.4$	6.69	0.6
$^{12}\text{C}$	$^{12}\text{B}$	$1^+$	0.0	$6.0 \pm 0.4$	0.0	6.0
		$2^+$	0.95	$0.21 \pm 0.10$	0.76	0.25
		$2^-$	1.67	$0.18 \pm 0.10$	1.49	0.22
		$1^-$	2.62	$0.62 \pm 0.20$	1.99	1.86

<sup>a</sup>Based on a 50% admixture between the  $0\hbar\omega$  and  $2\hbar\omega$   $2^+$  states.

tion. The resulting spin-dipole distribution is in good agreement with  $^{16}\text{O}(n,p)$  experiment (Fig. 8 in Ref. [25]).

The  $(0+2)\hbar\omega$  ground-state model also provides some GT strength to  $1^+$ ,  $T+1$  states in  $^{16}\text{O}$ . Our GT distribution and total strength (0.63) is similar to that obtained by Haxton and Johnson and appears to be about a factor of 2 smaller than observed in the  $^{16}\text{O}(p,n)$  [30] and  $^{16}\text{O}(n,p)$  [25] reactions (There is, however, a large uncertainty in the experiment due to background and the separation of the  $L=1$  and  $L=2$  multipoles). The GT strength in  $^{16}\text{O}$  is mainly important for the  $\mu^-$  capture where it contributes about 5 ( $\times 10^3/\text{s}$ ) to the total rate. Given its relatively small contribution and its large uncertainty the  $2\hbar\omega$  GT is not included in the final sum.

Our working model for weak interaction rates is to carry out the calculations in the  $0\hbar\omega$  ground-state model and then to multiply the results by 0.64. The reasons for not trying to apply the  $(0+2)\hbar\omega$  ground-state model to other nuclei are: (i) the calculations are much more difficult, (ii) there is no fully appropriate Hamiltonian for this space, and (iii) one should also include  $4\hbar\omega$  and the  $2s-1d-0g$  shell.

We wish to restate the factors that contribute to the reduction factor: (a) the RPA-type correlations reduce the strength due to the repulsive nature of the isovector particle-hole interaction; (b) other correlations due to the short-range part of the interaction that are also responsible for a reduction in the

absolute spectroscopic factors; (c) removal of strength in the spin channel due to the coupling to the  $\Delta_{33}$  resonance. Given that  $\gamma'$  may be attributed to all three factors whereas  $\gamma$  is usually only associated with (b) and (c), it is perhaps coincidental that  $\gamma' \approx \gamma$ . But within the framework of our  $0\hbar\omega$  ground-state model it is at least a convenient approximation.

The results for  $^{14}\text{N}$  are given in Table I. The  $\mu^-$  capture rate agrees well with our assumption of taking the  $0\hbar\omega$  result and multiplying by 0.64. The calculated DAR and DIF cross sections for  $^{14}\text{N}$  and  $^{16}\text{O}$  have not been measured. The  $0\hbar\omega$  results for  $^{12}\text{C}$  are given in Table I and Figs. 7–9. The DAR cross section, the  $\mu^-$  capture rate and the  $B(\text{GT})$  value are about 0.6 smaller in experiment than in the calculation. This is consistent with the analysis of the  $(p,n)$  [16,17],  $(p,p')$  [18],  $(e,e')$  [15,17], and  $(n,p)$  [19,20] data with the  $0\hbar\omega$  wave functions in which on the average only about half of the calculated cross section was observed. (We note, however, that there is some uncertainty in the analysis of the  $(p,n)$  and  $(n,p)$  reaction data. For example in Ref. [16], the quasifree background that is calculated to be about half of the total  $(p,n)$  cross section must be subtracted [16].)

The  $(0+2)\hbar\omega$  calculation for the GT transition in the  $p$  shell also reduces the strength. But this strength is very sensitive to the  $0\hbar\omega$  part of the wave functions. For example, it is well known [5] that the  $B(\text{GT})$  value obtained with a pure  $(0p_{3/2})^8$  configuration for  $^{12}\text{C}$  is a factor of 5 larger than the full  $p$ -shell value (given in Table I). Indeed, even the Coulomb interaction results in a 15% asymmetry between the  $^{12}\text{N}$  and  $^{12}\text{B}$   $B(\text{GT})$  values. (Our interactions and wave functions have good isospin and the  $B(\text{GT})$  values to these mirror states are equal in our model). The most reliable Hamiltonian we have at present for the GT strength is the WBP in the  $0\hbar\omega$  model space. It has been noted that the total dipole strength in  $^{12}\text{C}$  is insensitive to the structure of the  $0\hbar\omega$  ground state [31]. Thus, although the  $0\hbar\omega$  component of the  $(0+2)\hbar\omega$  mixed ground state may not be quite right, the calculation gives a good estimate for the amount of  $2\hbar\omega$  mixing and its effects on the higher multipole strengths.

For  $^{12}\text{C}$  the renormalized DAR cross sections,  $\mu^-$  capture rate, and  $B(\text{GT})$  values are all in good agreement with experiment. The calculated DIF cross sections are about 40% higher than experiment both for the ground state and the total. Since the ground-state strength (from the  $1^+$  state) agrees with the other data (DAR,  $\mu^-$  capture, and  $\beta$  decay), we could conclude that there is a systematic problem in the normalization of the DIF data. The smallness of the experimental DIF cross sections indicates that if a considerable amount of strength is shifted to higher energies by the quenching mechanism, most of it must lie above 100–150 MeV in the spectrum, otherwise it would be probed by the DIF neutrinos. Nuclear correlation calculations in heavy nuclei with  $N > Z$  indicate that the GT strength is shifted to higher excitation energy [32], but similar calculations have not been presented for light nuclei with  $N = Z$ . The axial-vector quenching may be related to the reduction in the spec-

troscopic factors observed in  $(e,e'p)$  reactions that is also attributed to short-range correlations [27].

In addition to the total  $\mu^-$  capture rates in Table I, we show the individual rates to the bound final states in Table II that have been measured by the observation of their  $\gamma$  decay following  $\mu^-$  capture [6,33]. One of the strongest of these is the transition to the  $^{12}\text{B}$   $1^+$  state discussed above. There is also a strong  $L=0$  transition from the  $^{14}\text{N}$   $1^+$   $T=0$  to the  $^{14}\text{C}$   $2^+$   $T=1$  state at 7.02 MeV [33]. There is a spread in the experimental rates (in units of  $10^3/\text{s}$ );  $2.2 \pm 0.9$  [33],  $4.6 \pm 0.7$  [34];  $10 \pm 3$  [35];  $8.0$  [36,37] and  $6.0 \pm 1.5$  [38,37]. The recommended average experimental value of  $4.4 \pm 0.6$  [33] is given in Table II. The next  $2^+$  state at 8.32 MeV is unbound to neutron decay. In our model there are low-lying  $2^+$  states at 6.85 and 7.77 MeV that have the structure  $2\hbar\omega$  and  $0\hbar\omega$ , respectively. The calculated  $\mu^-$  capture rates (the  $0\hbar\omega$  model with the 0.64 reduction factor) are 0 and 15 (all rates are in units of  $10^3/\text{s}$ ), respectively. These two  $2^+$  states are mixed by the off-diagonal interaction that is not included in the calculation. The  $^{14}\text{N}(n,p)$  data [39] indicates that the mixture is about 50-50. Thus, we would expect a  $\mu^-$  capture rate of about 7.5 to the lowest  $2^+$  state in fair agreement with the average experimental value. The other strong transition to bound states is for the transition from the  $^{16}\text{O}$  ground state to the  $^{16}\text{N}$   $2^-$   $T=1$  state where agreement with experiment is also fair. The other transitions compared in Table II are much weaker and the agreement between experiment and theory is good. For a few of the weak transitions the calculated partial rate is larger than experiment by about a factor of 2 to 3. We attribute this defect to the effective Hamiltonian (WBP) in which the distribution of  $L=1$  strength between these weak low-lying states and the stronger higher-lying “giant” resonance is given incorrectly in the model.

## VI. CONCLUSIONS

We have studied the weak processes  $(\nu_\mu, \mu)$ ,  $(\nu_e, e^-)$ ,  $\mu^-$  capture, and  $\beta$  decay in  $^{12}\text{C}$ ,  $^{14}\text{N}$ , and  $^{16}\text{O}$  in the framework of an extended shell-model space. Both exclusive transitions to the bound states of the final nuclei as well as the inclusive transitions summed over all final states have been computed. We have studied the dependence of the data considered on the quenching of the isovector strength. We find that the best overall agreement with experiment is obtained with a value of  $\gamma' = 0.8$ , which is close to that found for axial-vector GT transitions about 20 years ago,  $\gamma' \approx \gamma$ .

## ACKNOWLEDGMENTS

This work was supported by the U.S.-Israel Binational Science Foundation and by NSF Grant No. PHY-0070911. We wish to thank I. Towner for supplying the neutrino reaction and muon capture codes and D. F. Measday for sending us new results on  $\mu^-$  capture in  $^{14}\text{N}$ .



- [1] B. A. Brown and B. H. Wildenthal, *At. Data Nucl. Data Tables* **33**, 347 (1985). The  $B(\text{GT})$  as defined in the present work is related to the  $M(\text{GT})$  of this reference by  $B(\text{GT}) = [M(\text{GT})/1.251]^2/(2J_i + 1)$ .
- [2] F. Osterfeld, *Rev. Mod. Phys.* **64**, 491 (1992).
- [3] T. Wakasa *et al.*, *Phys. Rev. C* **55**, 2909 (1997).
- [4] B. A. Brown and B. H. Wildenthal, *Nucl. Phys.* **A474**, 290 (1987).
- [5] C. Volpe, N. Auerbach, G. Colo, T. Suzuki, and N. Van Giai, *Phys. Rev. C* **62**, 015501 (2001).
- [6] D. F. Measday, *Phys. Rep.* **354**, 243 (2001).
- [7] Nguyen Van Giai, N. Auerbach, and A. Z. Mekjian, *Phys. Rev. Lett.* **46**, 444 (1981).
- [8] N. Auerbach and A. Klein, *Nucl. Phys.* **A472**, 480 (1984).
- [9] KARMEN Collaboration, B. E. Bodman *et al.*, *Phys. Lett. B* **212**, 251 (1994).
- [10] LSND Collaboration, C. Athanassopoulos *et al.*, *Phys. Rev. C* **56**, 2806 (1997); C. Athanassopoulos *et al.*, *ibid.* **55**, 2078 (1997).
- [11] I. S. Towner (private communication).
- [12] A. C. Hayes and I. S. Towner, *Phys. Rev. C* **61**, 044604 (2001).
- [13] D. J. Millener and D. Kurath, *Nucl. Phys.* **A255**, 315 (1975).
- [14] E. K. Warburton and B. A. Brown, *Phys. Rev. C* **46**, 923 (1992).
- [15] R. S. Hicks *et al.*, *Phys. Rev. C* **30**, 1 (1984).
- [16] X. Yang *et al.*, *Phys. Rev. C* **52**, 2535 (1995).
- [17] B. D. Anderson *et al.*, *Phys. Rev. C* **54**, 237 (1996).
- [18] J. A. Templon *et al.*, *Phys. Lett. B* **413**, 253 (1997).
- [19] F. P. Brady *et al.*, *Phys. Rev. C* **43**, 2284 (1991).
- [20] N. Olsson *et al.*, *Nucl. Phys.* **A559**, 368 (1993).
- [21] M. Horjth-Jensen (private communication).
- [22] E. K. Warburton, B. A. Brown, and D. J. Millener, *Phys. Lett. B* **293**, 7 (1992).
- [23] H. Sagawa and B. A. Brown, *Phys. Lett.* **143B**, 283 (1984).
- [24] B. A. Brown, A. Etchegoyen, W. D. M. Rae, N. S. Godwin, W. A. Richter, C. H. Zimmerman, W. E. Ormand, and J. S. Winfield, MSU-NSCL Report No. 524, 1985 (unpublished).
- [25] K. H. Hicks *et al.*, *Phys. Rev. C* **43**, 2554 (1991).
- [26] A. Arima, K. Shimizu, W. Bentz, and H. Hyuga, *Adv. Nucl. Phys.* **18**, 1 (1987); I. S. Towner, *Phys. Rep.* **155**, 264 (1987).
- [27] D. Van Neck, L. Van Daele, Y. Dewulf, and M. Waroquier, *Phys. Rev. C* **56**, 1398 (1997).
- [28] L. Lapikas, G. van der Steenhoven, L. Frankfurt, M. Strikman, and M. Zhalov, *Phys. Rev. C* **61**, 064325 (2000).
- [29] W. T. Chu, E. K. Warburton, and B. A. Brown, *Phys. Rev. C* **47**, 163 (1993).
- [30] D. J. Mercer *et al.*, *Phys. Rev. C* **49**, 3104 (1994).
- [31] S. J. Robinson, L. Zamick, A. Mekjian, and N. Auerbach, *Phys. Rev. C* **62**, 017302 (2000).
- [32] G. F. Bertsch and I. Hamamoto, *Phys. Rev. C* **26**, 1323 (1982); D. Cha and J. Speth, *ibid.* **31**, 372 (1985); A. Klein, W. G. Love, and N. Auerbach, *ibid.* **31**, 710 (1985).
- [33] T. J. Stocki, D. F. Measday, E. Gete, M. A. Saliba, and T. P. Gorringe, *Nucl. Phys.* **A697**, 55 (2002).
- [34] M. Giffon *et al.*, *Phys. Rev. C* **24**, 241 (1981).
- [35] A. I. Babaev *et al.*, JINR Report R-14-42-41, 1968; quoted by V. A. Vartanyan *et al.*, *Sov. J. Nucl. Phys.* **11**, 295 (1970).
- [36] L. Genacs, quoted on p. 47 of [37].
- [37] N. C. Mukhopadhyay, *Phys. Rep.*, *Phys. Lett.* **30C**, 1 (1977).
- [38] E. Belloti *et al.*, *SIN Newsletter* **1C**, 41 (1976) and quoted on pp. 58 and 131 of [37].
- [39] K. P. Jackson *et al.* (private communication).
- [40] T. J. Stocki and D. F. Measday (private communication).
- [41] J. P. Perroud *et al.*, *Nucl. Phys.* **A453**, 542 (1986).